DOI: 10.1111/cgf.14306
Eurographics Conference on Visualization (EuroVis) 2021
R. Borgo, G. E. Marai, and T. von Landesberger
(Guest Editors)

Volume 40 (2021), Number 3

SenVis: Interactive Tensor-based Sensitivity Visualization

Haiyan Yang[1], Rafael Ballester-Ripoll[2], and Renato Pajarola[1]

[1]Department of Informatics, University of Zürich
[2]IE School of Human Sciences and Technology

Abstract

Sobol's method is one of the most powerful and widely used frameworks for global sensitivity analysis, and it maps every possible combination of input variables to an associated Sobol index. However, these indices are often challenging to analyze in depth, due in part to the lack of suitable, flexible enough, and fast-to-query data access structures as well as visualization techniques. We propose a visualization tool that leverages tensor decomposition, a compressed data format that can quickly and approximately answer sophisticated queries over exponential-sized sets of Sobol indices. This way, we are able to capture the complete global sensitivity information of high-dimensional scalar models. Our application is based on a three-stage visualization, to which variables to be analyzed can be added or removed interactively. It includes a novel hourglass-like diagram presenting the relative importance for any single variable or combination of input variables with respect to any composition of the rest of the input variables. We showcase our visualization with a range of example models, whereby we demonstrate the high expressive power and analytical capability made possible with the proposed method.

Keywords: Sobol indices, tensor-based sensitivity computation, explorative sensitivity analysis, interactive sensitivity visualization

CCS Concepts

• **Human-centered computing** → **Visualization;** • **Theory of computation** → **Design and analysis of algorithms;**

1. Introduction

One of the most central goals when exploring and visualizing a parametrized model is quantifying its sensitivity to the variability of its input variables. This is a challenging task, even for domain experts, and even more so if we wish to query and visualize those sensitivities in an interactive way. To make matters worse, key insights about the model may arise only when studying specific *interactions* between two or more variables. While a first-order analysis of, say, an epidemiological model may separately identify the most influential variables that affect the spread of a disease, a higher-order analysis will crucially reveal which *combinations* of variables are important.

To approach such types of questions, global sensitivity analysis (GSA) [SRA*08] has proven to be a powerful tool to assess the significance of the input variables for computational models and simulations which are quadratically integrable functions with mutually independent variables. A common form of variance-based GSA, often referred to as *analysis of variances* (ANOVA), is the so-called *Sobol decomposition* [Sob90]. It approximates an N-dimensional model as a sum of simpler functions, each depending only on a specific subset of the original set of N variables. The sensitivity to each single as well as any combination of input variables can then be estimated as its relative contribution to the output's overall statistical variance. These relative variances have become a standard tool for GSA [SRA*08, Sud08, IL15].

While our work is related to set-typed data visualization, hypergraph visualization and uncertainty quantification, it nevertheless addresses a unique problem setting which no previous approach directly applies to. We consider here deterministic models only (that is, those that produce a unique guaranteed output for each input). Therefore, given a multidimensional model with N input parameters we consider mappings of the form

$$S : \mathcal{P}(\{1,...,N\}) \to \mathbb{R}, \tag{1}$$

where $\{1,\dots,N\}$ is the set of input parameters or variables and $\mathcal{P}$ is the *power set* operator, i.e., S is defined on *every possible subset* of $\{1,\dots,N\}$ of which 2^N exist. For GSA, the mapping S measures the importance or uncertainty of an arbitrary variable subset, any possible element of $\mathcal{P}$, on the output of the model.

The visualization of GSA poses two unique challenges. The first is the exponential growth of its domain: a mapping of all subsets of $\{1,\dots,N\}$ results in 2^N outputs, being the size of $\mathcal{P}$, each of which may be hard to compute. The second challenge is then querying and visualizing all types of corresponding sensitivity indices, as the interactive visual exploration of all their mutual relations can be hard and has not been well studied yet.

© 2021 The Author(s)
Computer Graphics Forum © 2021 The Eurographics Association and John Wiley & Sons Ltd. Published by John Wiley & Sons Ltd.

delivered by EUROGRAPHICS DIGITAL LIBRARY www.eg.org diglib.eg.org

To tackle the aforementioned challenges, we organize the sensitivity Sobol indices as a hypercube of size 2^N as illustrated in Fig. 1. In this format, querying any Sobol indices is equivalent to manipulating hypercube slices in various ways, as we will outline in more detail in Sec. 3. To deal effectively with the exponential 2^N subset configurations, we use a compressed tensor data structure to represent this hypercube and to compute all four types of Sobol indices efficiently. This representation enables four main contributions which are integrated into the proposed visualization system:

1. We have developed the first interactive visualization application centered around Sobol sensitivity indices.
2. We are, to the best of our knowledge, the first to adapt set related visualization techniques to global sensitivity analysis.
3. We propose two novel quantities of interest, the relative importances and directional covariances, that assist in the analysis of the sensitivity indices.
4. We leverage a tensor-based data structure that, besides holding an exponential number of indices, allows us to extract more advanced derived metrics and query them in real time.

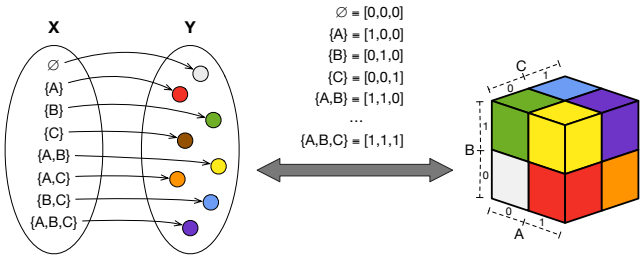

Figure 1: *A Sobol index tensor for a function with three ($N = 3$) input variables A, B, and C can be understood as arranging 2^N objects, all possible variable subsets (left), to form an N-dimensional hypercube (right).*

2. Related Work

2.1. Global Sensitivity Analysis

The Sobol decomposition [Sob90], also known as high-dimensional model representation (HDMR) [BEK15] or ANOVA decomposition [ES81] is one of the most important and widely used variance-based GSA approaches. The Sobol decomposition writes any squared-integrable multidimensional function $f : \mathbb{R}^N \to \mathbb{R}$ as a sum of subfunctions:

$$f(\boldsymbol{x}) = f_\emptyset + \sum_{i=1}^{N} f_i(x_i) + \sum_{1\le i<j\le N} f_{ij}(x_i,x_j) + \cdots$$
$$\cdots + \sum_{\substack{\boldsymbol{\alpha}\subset\{1,\ldots,N\}\\ |\boldsymbol{\alpha}|=n}} f_{\boldsymbol{\alpha}}(x_{\boldsymbol{\alpha}}) + \cdots + f_{1,\ldots,N}(x_1,\ldots,x_N),$$

where each subfunction $f_{\boldsymbol{\alpha}}$ only depends on the indices contained in $\boldsymbol{\alpha} \subseteq \{1,\ldots,N\}$. We denote tuples of indices as $\boldsymbol{\alpha} \in \{0,1\}^N$ or $\boldsymbol{\alpha} \subseteq \{1,\ldots,N\}$ interchangeably: a 0 (or 1) in the former notation means an index is absent (or present) in the latter. For a 4-dimensional function $f : \mathbb{R}^4 \to \mathbb{R}$ we may thus write $\boldsymbol{\alpha} = (0,0,1,1)$ or $\boldsymbol{\alpha} = \{3,4\}$ to refer to the two last variables, similar to [Sud08, Owe14].

Given the variance $D = \mathrm{Var}[f]$ of a model f over its entire domain, the Sobol decomposition splits it up into a partition $D = \sum_{\boldsymbol{\alpha}} V_{\boldsymbol{\alpha}}$ of variances induced by different groups of variables $\boldsymbol{\alpha} \in \{0,1\}^N$. The *Sobol indices* $S_{\boldsymbol{\alpha}}$ arise from normalizing the $V_{\boldsymbol{\alpha}}$ by the total variance D, i.e., are a mapping $S : \mathcal{P}(\{1,\ldots,N\}) \to [0,1]$:

$$S_{\boldsymbol{\alpha}} := V_{\boldsymbol{\alpha}}/D \text{ with } \sum_{\boldsymbol{\alpha}} S_{\boldsymbol{\alpha}} = 1$$

These indices are an invaluable tool in many GSA settings [STCR04], for example in factor prioritization (reducing uncertainty), factor fixing (identifying non-influential variables), risk minimization, reliability engineering, etc. They are also helpful to select good dimension orderings that lead to more compact surrogate models (example 5.8 by Bigoni [BEK15]; also considered in [DKLM14]). They are hyperedges of a hypergraph, since they encode n-ary relations within subsets of $\{1,\ldots,N\}$. Alternatively, they can also be thought of in terms of set cardinalities, as the sum of all $S_{\boldsymbol{\alpha}}$ equals 1 (see e.g., [Owe13] and [SRA*08], Sec. 1.2.15).

In addition to the standard Sobol indices $S_{\boldsymbol{\alpha}}$ for all possible subsets of variables $\boldsymbol{\alpha} \in \mathcal{P}$, there are further derived indices based on adding or subtracting the standard indices, corresponding to a set algebra on the variables as further explained in Sec. 3.2.

A popular method to compute such indices is using *Monte Carlo* (MC) integration [Sob90]. But since MC converges slowly with respect to the number of required samples [IL15], improved methods have been proposed [WWO*17]. In practice, the Sobol decomposition is often restricted to interactions between only few variables, e.g., up to two, for performance reasons. Complementary approaches build a *surrogate model*, e.g., using Gaussian processes [KSV*15] or radial basis functions [WWO*16], which approximates the true unknown model [QHS*05]. Certain surrogate models can be used to extract Sobol indices directly without MC integration [IL15, WWO*16]. Nevertheless, coping with a larger number N of input variables remains challenging. Even if the surrogate scales well with the dimensionality [KS16], the number of sensitivity indices grows exponentially, in the order of 2^N.

To avoid these problems, we use a tensor approximation based representation of the Sobol indices [BRPP18, BRPP19]. In contrast to other approaches, which can compute individual or aggregated sensitivity indices from surrogates [Rai14, DKLM14, KS16], the tensor based approach allows to represent and query the complete set of all possible indices in a compact form. In this work, we build a visualization system on top of that idea.

2.2. Uncertainty and Set Visualization

While uncertainty quantification (UQ) and visualization has been well studied [PRJ12, HQC*19], very few methods aim at visualizing *calculated* metrics of uncertainty. However, such metrics are central in countless communities (risk management, structural reliability in engineering, system safety, scientific computing, etc.) when they refer to *UQ*. Existing visualizations favor visual encodings rather than explicitly displaying auxiliary calculated quantities. While feasible for data of limited dimensionality, such direct visual approaches

© 2021 The Author(s)
Computer Graphics Forum © 2021 The Eurographics Association and John Wiley & Sons Ltd.

become much less viable for N-dimensional parameter spaces. For example, Biswas et al. [BLLS16] studied the uncertainty of weather ensembles for spatial and temporal regions using only one global sensitivity measure called *delta* and for only three dimensional data.

Among the methods that do quantify uncertainty metrics, many actually deal with uncertainties in the data underpinning the model in question [BHJ*14]. Others consider stochastic parameter spaces instead, as multiple realizations of some experiments or simulations may yield disparate outcomes that need to be accounted for in the visualization. In contrast, in this paper we focus on the variability of the parameters as the critical source of uncertainty of a deterministic and accurate model. In the particular case where that variability is not random we fall into the realm of sensitivity analysis, i.e., we want to study the influence of freely *tunable* parameters on the model's output. To the best of our knowledge, the only visualization ever proposed to specifically display Sobol indices is the *fanovaGraph* [FRM13], which uses static radial graphs to compactly display indices, but only of order up to two.

Several well-established diagrams and visualization systems are dedicated to generic set and set-typed data including *Radial Sets* [AAMH13], *OnSet* [SMDS14], *PivotPaths* [DHRRD12], and *UpSet* [LGS*14]. Sets can be cast as hypergraphs [VBP*19], which has resulted in a symbiosis with the growing field of graph drawing and network visualization. Alsallakh et al. [AMA*14] summarized the state-of-the-art set visualization techniques and categorized the field's standard requirements in the form of 26 types of tasks that can be performed over sets, their elements, and their attributes. Even though Sobol indices are interpretable as set cardinalities, (i) they are continuous in nature and can only be regarded as infinite sets, (ii) they do not make any reference to set elements, and (iii) there are no individual elements whose attributes need to be displayed. Therefore, Sobol indices and their visual analysis are significantly different from generic set visualizations. In addition, since Sobol indices naturally combine with each other to yield *superset*, *closed*, and *total* indices, each with its particular interpretation (Sec. 3.2), we need to visualize *several* interaction relationships at the same time. Combined, the requirements for variance-based GSA visualization form unique challenges that have not been addressed before.

3. Tensor Decompositions for Sensitivity Analysis

3.1. Sobol Tensor Model

We use data tensors (N-dimensional arrays) to represent parameter spaces. For GSA, we use tensors of size 2^N to encode variable interactions of *all* possible orders $1,\dots,N$. Due to the *curse of dimensionality*, the power set $\mathcal{P}$ over all possible N variables grows exponentially with the number N of elements. For example, all Sobol indices $S_{\boldsymbol{\alpha}}$ over 30 variables, where $\boldsymbol{\alpha} \in \{0,1\}^{30}$, require several gigabytes. The goal of tensor decompositions is to handle large and complex data tensors in a *linearly transformed* and often *compressed* format. However, instead of predefining the transform bases (such as e.g., in the cosine or wavelet transforms), tensor decompositions find *data-dependent* bases that can compress much more effectively (especially for high dimensions).

This idea is a higher-order generalization of the reduced-rank SVD matrix approximation [KB09]. Recently, it has been used to compress and interactively visualize multidimensional scalar fields [BRP16]. In contrast to such scalar fields, that often have low dimensionality (e.g., $N = 3$ or 4) but large resolutions (e.g., 1000s of indices per dimension), the Sobol indices in variance-based GSA constitute a high-dimensional data tensor (with N up to several 10s) of low resolution (index being $\{0,1\}$). For further details on tensor decompositions, we refer the reader to the supplementary material.

To efficiently represent Sobol index tensors of size 2^N, we use the *tensor train* (TT) format [Ose11], which is very efficient for high dimensionality N. It uses a sequence of N *tensor cores* $\mathcal{T}^{(n)}$, compactly written as $[[\mathcal{T}^{(1)},\dots,\mathcal{T}^{(N)}]]$. Except for the first and last tensors $\mathcal{T}^{(1)}$ and $\mathcal{T}^{(N)}$, which consist of two row or column vectors of length R_1 and R_{N-1} respectively, all other tensor cores $\mathcal{T}^{(n)}$ consist of 2 slices of $R_{n-1} \times R_n$ matrices each as shown in Fig. 2.

Suppose we are interested in a certain tuple of attributes $\boldsymbol{\alpha}$, and let us write $\boldsymbol{\alpha} \equiv (\alpha_1,\dots,\alpha_N)$ where $\alpha_n = 1$ if $n \in \boldsymbol{\alpha}$ and 0 otherwise. For instance, $\boldsymbol{\alpha} = \{2,3\}$, with $N = 3$ this equates to $(0,1,1)$. Since each core $\mathcal{T}^{(n)}$ consists of two matrices, the first one, denoted as $\mathcal{T}^{(n)}[0]$, encodes the case $n \notin \boldsymbol{\alpha}$, while the second one, $\mathcal{T}^{(n)}[1]$, encodes the case $n \in \boldsymbol{\alpha}$. Using the TT format, to query a mapping S as in Eq. 1 on a certain tuple $\boldsymbol{\alpha}$ we just need to perform a sequence of N matrix-matrix multiplications:

$$S_{\boldsymbol{\alpha}} \approx \mathcal{T}^{(1)}[\alpha_1] \cdot \ldots \cdot \mathcal{T}^{(N)}[\alpha_N]$$

Fig. 2 illustrates the structure and indexing of a Sobol TT core sequence for $N = 7$ and tensor ranks $R_1 \dots R_6$. For more details on the definition, construction and use of Sobol TTs we refer the interested reader to [BRPP19].

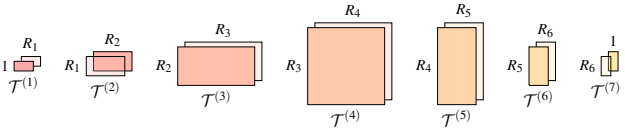

Figure 2: *Sobol indices S for a 7D function ($2^7 = 128$ indices in total) compactly stored in the TT format representing a tensor $\mathcal{T}$ of size 2^7. For instance, $S_{\{2,7\}}$ is given as the tensor element $\mathcal{T}_{\{2,7\}} = \mathcal{T}[0,1,0,0,0,0,1]$, which is decompressed by multiplying the 7 highlighted matrices together.*

Moreover, since the first and last matrices $\mathcal{T}^{(1)}$ and $\mathcal{T}^{(N)}$ are row and column vectors, respectively, the sequence actually consists of simple vector-matrix products and is thus highly efficient. Each access of a Sobol index $S_{\boldsymbol{\alpha}}$ requires constant time independently of the number k of selected variables in $\boldsymbol{\alpha}$. Therefore, we are able to keep up with the performance needs of an interactive visualization application, and we can query and retrieve hundreds of Sobol indices per second using this representation. Crucially, this format is free from the curse of dimensionality as it grows linearly, not exponentially, w.r.t. N.

A Sobol TT $\mathcal{S}$ as outlined above can efficiently represent the whole space of all 2^N Sobol indices as a surrogate model. The numerical approximation quality, and memory cost, of a TT-compressed Sobol tensor $\mathcal{S}$ depends on the number of tensor ranks $R_1 \dots R_{N-1}$.

© 2021 The Author(s)
Computer Graphics Forum © 2021 The Eurographics Association and John Wiley & Sons Ltd.

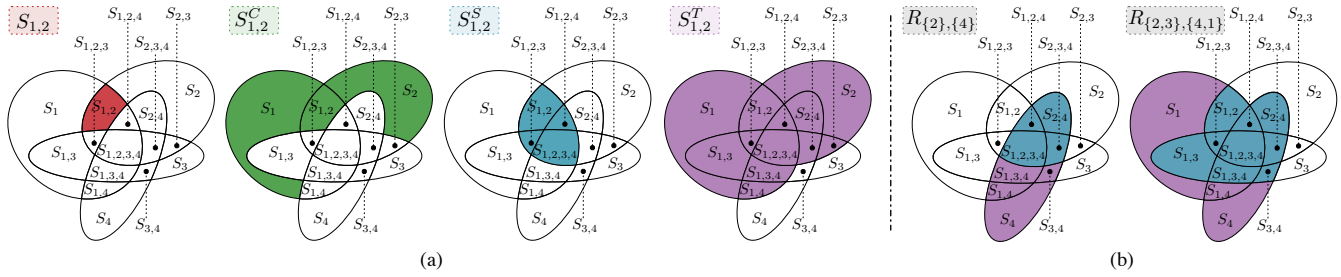

Figure 3: *Illustration of Sobol indices and relative importance for a four-variable case. (a) Sobol, closed, superset and total indices of a variable pair* $\boldsymbol{\alpha} = \{1,2\}$*, out of four variables. (b) Example of different relative importances, equivalent in each case to the sum of Sobol indices in the blue area divided by their sum over blue plus purple areas.*

Modest ranks are often enough to attain high accuracy: in the models tested in this paper, a rank of 16 was enough to keep the root mean squared error (RMSE) below 10^{-6} (see also Sec. 7).

3.2. Accessing Sobol Indices

Due to its multilinearity we can easily compute and visualize a wide variety of operations connected to variable selections for functions represented in the TT format [BRPP19]. The most standard query, reading out one Sobol index, is accomplished via a sequence of vector-matrix products. Other derived indices follow from applying set algebra operations in the tensor compressed domain, including:

Closed Indices: For every tuple $\boldsymbol{\alpha}$, its *closed index* $S^C_{\boldsymbol{\alpha}}$ [Owe13] sums the contributions of the Sobol indices of all non-empty subsets contained in $\boldsymbol{\alpha}$, formally: $S^C_{\boldsymbol{\alpha}} := \sum_{\boldsymbol{\beta}|\boldsymbol{\beta}\subseteq\boldsymbol{\alpha}} S_{\boldsymbol{\beta}}$.

Superset Indices: The *superset index* $S^S_{\boldsymbol{\alpha}}$ [Hoo04] of a tuple $\boldsymbol{\alpha}$ is the aggregated sum of all tuples containing $\boldsymbol{\alpha}$: $S^S_{\boldsymbol{\alpha}} := \sum_{\boldsymbol{\beta}|\boldsymbol{\beta}\supseteq\boldsymbol{\alpha}} S_{\boldsymbol{\beta}}$.

Total Indices: The *total index* $S^T_{\boldsymbol{\alpha}}$ [Owe13] of a tuple $\boldsymbol{\alpha}$ is the sum of all tuples that are not disjoint from it: $S^T_{\boldsymbol{\alpha}} := \sum_{\boldsymbol{\beta}|\boldsymbol{\beta}\cap\boldsymbol{\alpha}\neq\emptyset} S_{\boldsymbol{\beta}}$.

All four indices form a powerful toolset for a range of modeling tasks [STCR04], each of them finds different uses in model screening and simplification, factor prioritization, risk minimization, etc. For example, the total indices allow an analyst to identify non-influential variables and remove them by *freezing* them to specific values. Fig. 3 (a) graphically illustrates the four types of indices for a 4D model using Venn diagrams.

3.3. Relative Importances

The Sobol and its derived indices only target the direct influence due to each variable tuple. We propose an additional tool to further relate index aggregations with each other, the *relative importance* of a tuple of variables $\boldsymbol{\alpha}$ with respect to another tuple $\boldsymbol{\beta}$, defined as

$$R_{\boldsymbol{\alpha},\boldsymbol{\beta}} = \frac{\sum_{\boldsymbol{\gamma}|\boldsymbol{\gamma}\cap\boldsymbol{\alpha}\neq\emptyset,\ \boldsymbol{\gamma}\cap\boldsymbol{\beta}\neq\emptyset} S_{\boldsymbol{\gamma}}}{\sum_{\boldsymbol{\gamma}|\boldsymbol{\gamma}\cap\boldsymbol{\beta}\neq\emptyset} S_{\boldsymbol{\gamma}}}. \tag{2}$$

The relative importance index $R_{\boldsymbol{\alpha},\boldsymbol{\beta}}$ measures what fraction of the overall effect of $\boldsymbol{\beta}$ is actually due to its interactions with variables in $\boldsymbol{\alpha}$, and it allows us to breakdown joint effects into their building blocks. Thus, it is particularly helpful for exploring relations between two variable tuples (see also Sec. 5.1.3). This new metric can be seen as the GSA equivalent of the concept of conditional probability of an event A given another event B, $P(A|B) = \frac{P(A\cap B)}{P(B)}$. See Fig. 3 (b) for a corresponding illustration.

3.4. Directional Covariances

Being variance-based, Sobol indices and their variants communicate the strength of an effect in *absolute* terms but do not take into account its sign. For example, we may see that increasing one or several variables exerts a large influence on the model output, but not whether that effect is positive (i.e., leads to an *increase* of the model's output), negative (leads to a *decrease*), or mixed.

In order to convey this important information, we propose and visualize what we denote as *directional covariances*: for every set of variables $\boldsymbol{\alpha} = \{i_1,\ldots,i_k\}$, being the covariance

$$C_{\boldsymbol{\alpha}} := \mathrm{cov}(\mathbb{E}_{\overline{\boldsymbol{\alpha}}}[f], x_{i_1} + \cdots + x_{i_k})$$

where the expectation of f is taken over the domain of all variables outside $\boldsymbol{\alpha}$, i.e., its complement $\overline{\boldsymbol{\alpha}}$.

Intuitively, $C_{\boldsymbol{\alpha}}$ measures the correlation between the model of interest $f(\boldsymbol{x})$ and the function $x_{i_1} + \cdots + x_{i_k}$, i.e., quantifies how much the model increases (or decreases) when we increase variables $i_1,\ldots,i_k$ simultaneously. A positive $C_{\boldsymbol{\alpha}}$ means the model output generally grows when we increase all variables in $\boldsymbol{\alpha}$ at once, and conversely, a negative $C_{\boldsymbol{\alpha}}$ tells us $f(\boldsymbol{x})$ shrinks as we decrease them. This quantity is useful in model understanding tasks that benefit from knowing the sign of variable influences. One typical example is presented in the Ebola spread model in Sec. 6.1.

4. GSA Tasks and Visual Requirements

To effectively support the interactive visual exploration of variance based GSA metrics like Sobol indices (HDRM or ANOVA decomposition), two challenging tasks have to be addressed. These tasks are to access and extract the set of all Sobol indices efficiently, and to get an understanding of the Sobol indices in an effective way. While Sobol index querying is well addressed by applying the Sobol

© 2021 The Author(s)
Computer Graphics Forum © 2021 The Eurographics Association and John Wiley & Sons Ltd.

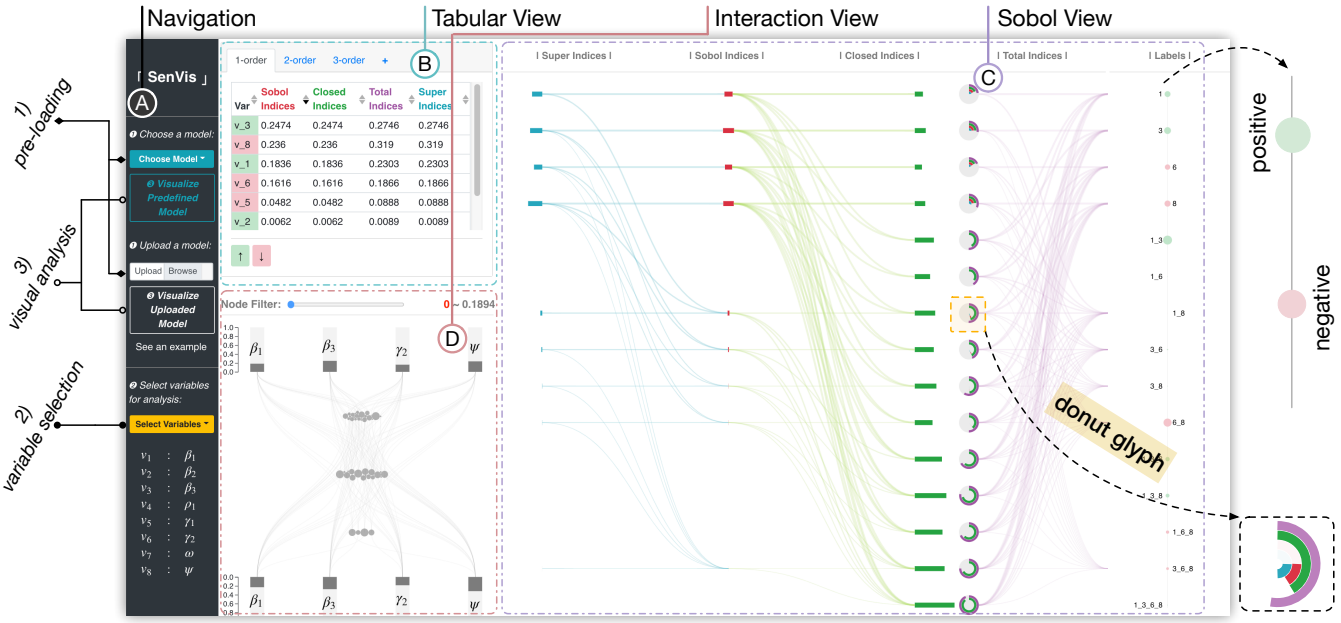

Figure 4: *SenVis system overview for Ebola spread model with* 8 *variables originally, out of which* 4 *variables are recognized and selected from the navigation bar A as* important *by looking up the order-*1 *Sobol indices values from tabular view B, then all four types of sensitivity indices up to order 4 are visualized in two interactive visualization diagrams C (Sobol view) and D (interaction view) to help users gain a comprehensive understanding of the model's input variables.*

TT decomposition method [BRPP19], the second task requires an interactive tool to visually show the interaction between Sobol indices and how they affect each other in any dimension. To achieve this, we identified the following essential requirements as a visual design guidance:

R1: The system should be able to access all four types of sensitivity indices instantly up to a given order k, and allow the user to quickly explore the larger indices of any type and order $d \leq k$.

R2: Considering the possible high dimensionality of a model and relatively limited number of effective input variables, the system should be able to visualize specifically the variables of interest interactively. This is also crucial for preventing potential visual clutter problems.

R3: To help understanding the importance of each combination of input variables, a visual diagram presenting the relations among all four types of sensitivity indices is needed for a better user experience.

R4: Assisting users to gain a deep knowledge about the interaction of each variable or variable pair with respect to the rest of the variables is critical for tasks like model understanding and model simplification. For example, when a variable has little interaction with all the other variables, it is reasonable to reduce the model complexity by fixing or limiting the choice of this variable. Conversely, a variable that has a significant interaction with some or all of the rest of the variables should be treated carefully.

R5: The system should be flexible to analyze user-defined models.

5. Proposed Visualization

To fulfill all the visual design requirements efficiently and effectively, we have built a three-stage visualization system *SenVis* which includes a server side handling all the computation tasks (such as Sobol tensor construction and sensitivity indices calculation) and a client side serving the web-based interactive visualization interface consisting of four components: navigation bar, *tabular view*, *Sobol view* and *interaction view* as shown in Fig. 4.

5.1. System Overview

SenVis addresses requirements R1-R5 as follows:

1) Pre-loading: Select or upload the desired model in the navigation bar, then the server side will calculate the complete (or semi-complete up to a limited order k) collection of sensitivity indices and send it to the client side, as well as display it in a lookup table called *tabular view* (**R1**). For moderately complex models and $N \leq 10$, the computation takes less than 5 seconds.

2) Variable Selection: Choose the variables of interest (**R2**) after examining all the Sobol indices in the order that is important for the analytical tasks and select them in the navigation. Then trigger the visualization which includes a second round of computations specifically for the selected variables needed to drive the different visualization widgets. In practice, to prevent visual clutter, it is recommended to choose less than 8 variables simultaneously. The user can repeatedly do variable selections to gain a comprehensive view over the input variable space in case some of the variables trigger one's interest for further exploration.

© 2021 The Author(s)
Computer Graphics Forum © 2021 The Eurographics Association and John Wiley & Sons Ltd.

3) Visual Analysis: Two visualization diagrams will be displayed after loading and computing (depending on the number of chosen variables): The *Sobol view*, which visualizes the detailed relation of four types of sensitivity indices in one integrated and interactive linked diagram (**R3**), and the *interaction view*, which helps to reveal the high-dimensional entangled relative relations of any two disjoint subsets of the original variable space using a novel hourglass visualization (**R4**).

5.1.1. Tabular View

The *tabular view* is generated in the pre-loading phase and will not change until a new model is either chosen or uploaded through the navigation bar (Fig. 4 A).

As can be seen in Fig. 4 B, it is a five-column table with the first column indicating the variables' labels colored in light green or red corresponding to their positive or negative *directional covariance*, respectively. The other four columns indicate the corresponding first order *Sobol* (red), *closed* (green), *total* (purple) and *superset* (blue) indices. Users can easily add and navigate higher order sensitivity indices as well as remove them again, by clicking the "+" symbol on the top of the table or by pressing the "close" button at the bottom right for higher orders tabs respectively. Moreover, all the columns are sortable, thus providing a convenient exploration and quick variable targeting for variable selection (**R1**).

After pre-loading, the user can sort the first order indices based on Sobol or total indices and pick the most influential ones (**R2**), which typically are the ones with larger values, from the variable selection option in the navigation bar (Fig. 4 A). Then the visual diagrams will be generated after clicking the *visualize selected* or *uploaded model* button, corresponding to the chosen selection of variables as needed for the visual analysis task at hand.

5.1.2. Sobol View

The *tabular view* is not expressive enough to help understand how the derived indices are related to the basic Sobol indices as outlined in Sec. 3.2. To have a more general picture of the model's input variables in first- and higher-order Sobol form and to gain a complete relation graph of all the sensitivity indices, we designed the *Sobol view* (**R3**) as shown in Fig. 4 C as a parallel linked diagram where *superset* (blue), *Sobol* (red), *closed* (green) and *total* (purple) indices $S^S_{\boldsymbol{\alpha}}$, $S_{\boldsymbol{\alpha}}$, $S^C_{\boldsymbol{\alpha}}$ and $S^T_{\boldsymbol{\alpha}}$ for each variable tuple $\boldsymbol{\alpha}$ are visualized.

On the left side of Fig. 4 C, the horizontal bar lengths show the value of the corresponding indices, and the weighted curved links express the relation between two adjacent bars. The weights of the links correspond to the contributing value of the basic Sobol indices to the derived ones, so the smaller the Sobol index's contribution the thinner the link. We can see how the Sobol indices (from the center) contribute to the superset (to the left) as well as closed (to the right). On the right side of Fig. 4 C, the total indices are succinctly visualized as four-arc concentric donut charts. The circular arcs depict how the total index is composed of the closed, Sobol, and superset indices (outside-in, same order as when reading the horizontal bars from right to left.) with the angle of the arc segment representing the contributing value. The curves link to the variable sets $\boldsymbol{\alpha}$ in the *Labels* column, where additionally their directional covariance $C_{\boldsymbol{\alpha}}$ is given by the bubble size and its positive or negative effect indicated by color and with the labels on the left or right respectively.

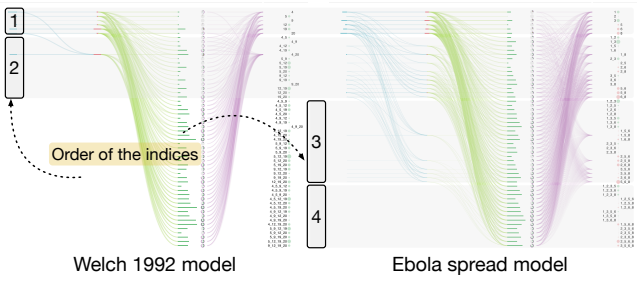

Figure 5: *Sobol view: The Sobol indices of the* 20*-dimensional Welch 1992 model have a clear second-order cutoff, while the Ebola spread model exhibits more higher order interactions.*

From the simple yet powerful visual representation of Sobol's relations, we can gain a coarse-to-fine understanding of the behavior for all variable tuples. For instance, as demonstrated in Fig. 5 we can observe a clear difference between two models, where one model has a clear second-order cutoff while the other shows a higher-order variable influence. This indicates that the second model is more complex since also higher-order Sobol indices take a noticeable amount of influence to the model output, likely preventing an easy simplification of it into lower-order approximations without much loss of model variability.

To support precise information exploration, three types of interactions are integrated for all four index types as illustrated in Fig. 6. For each variable tuple, *hovering* over its superset, Sobol, or closed bar chart triggers the highlighting of a) the superset, Sobol, and closed indices values below the bars, b) its total donut with the corresponding arc highlighted, and c) all the labels that contribute to its total index. Hovering over its total donut chart triggers the highlighting of the variable bubble charts that contribute to it with colored links.

Second, *clicking* on a Sobol index bar chart triggers highlighting its links in red, showing its contributions to other superset and closed indices. Clicking on either a superset or closed index bar chart triggers highlighting blue or green links showing its composition from Sobol indices, which is difficult to imagine and visualize via standard set operations. Moreover, by selecting multiple bar charts, users can compare the composition of two or more Sobol indices in detail.

Third, *hovering* over a total index donut chart causes a tooltip to appear showing its full composition, assisting in the understanding of it especially when the effect of other than superset, Sobol or closed indices is not known in any other view explicitly. Eventually, double clicking on any bar chart can always reset this view into the default state and start a next round of exploration.

Other visual design alternatives, like arc [Wat02], chord [Hol06] or Sankey diagrams [RHF05], and matrix techniques [SMDS14], each have their advantages, but also limitations. Both arc and chord diagrams can be used for linking relations between different sensitivity indices but suffer from unused (blank) space around big

© 2021 The Author(s)
Computer Graphics Forum © 2021 The Eurographics Association and John Wiley & Sons Ltd.

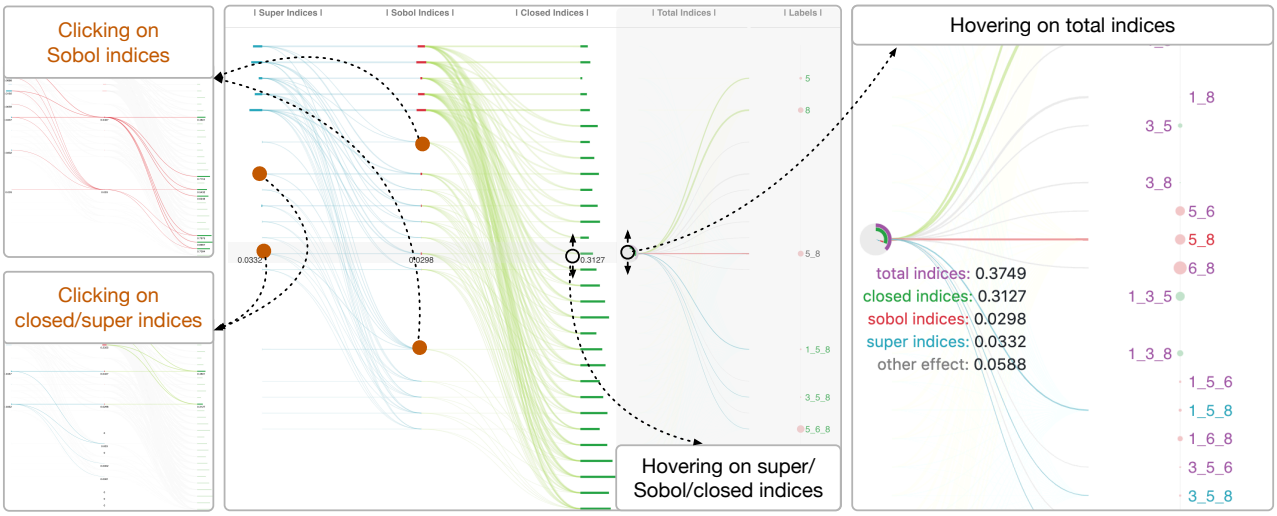

Figure 6: *Annotated Sobol view indicating the various possible interaction options.*

arcs. Furthermore, comparing the value of all indices is difficult as the Sobol indices could be encoded as the fragments of arcs and either height or width, both difficult for comparative analysis. Sankey diagrams are common for flow visualization, however, they do not fit the Sobol context because the different types of sensitivity indices do not have a corresponding flow structure or transformation relation which is key for this visual representation. Matrix diagrams have a determinative limitation of not being able to compare more than two sets at one time.

5.1.3. Interaction View

The *Sobol view* extends the *tabular view* in the way that relations between superset (closed, total) indices and Sobol indices for every variable tuple are visualized compactly in one view, thus can be easily explored and compared. However, there are some key questions it cannot answer, which is important for the understanding of the inter-relation of all the input variables with or without prior knowledge and the model simplification task (find and remove less important variables) (**R4**).

For example, what is the relative importance of attribute 1 with respect to the variable tuple $\boldsymbol{\beta} = \{2,3\}$? And more generally, what is the relative importance of any variable tuple $\boldsymbol{\alpha} \subseteq \{1,...,N\}$ with respect to any other variable tuple $\boldsymbol{\beta} \subseteq \{1,...,N\} \setminus \boldsymbol{\alpha}$, hence with $\boldsymbol{\alpha} \cap \boldsymbol{\beta} = \emptyset$? Second, finding out which variable tuple is more important can be done by quickly examining its total index in the *tabular view*. However, knowledge about which variables inside of that tuple share more *interaction effect* with other variables remains unknown. This type of insight is critical in determining whether removing a certain variable or not will keep the simplified model close enough to the original higher-order one. This is because variables which have little interaction with others do not affect other variables' sensitivity behavior.

These types of questions can be answered and explored in our *interaction view* as shown in Fig. 4 D which we call *hourglass graph*. There are three main elements to visualize in this view, the two disjoint variable tuples $\boldsymbol{\alpha}$ and $\boldsymbol{\beta}$, and their relative importance as defined in Eq. 2 in Sec. 3.3. For example, for $\boldsymbol{\alpha} = \{1\}$ we want to visualize the relative importance $R_{\boldsymbol{\alpha},\boldsymbol{\beta}}$ to $\boldsymbol{\beta} \subseteq \{2,3,4\}$ for $N = 4$.

A scatter plot is a natural way to visualize the relative importance contributions by encoding them with the size of bubbles. Furthermore, to make the space usage more efficient and the structure of $R_{\boldsymbol{\alpha},\boldsymbol{\beta}}$ clearer, we adopt a *force layout bubble* chart technique and vertically cluster bubbles into groups based on the cardinality of $\boldsymbol{\alpha}$. For example, if five variables are selected for visualization in the variable selection phase, the bubbles will be grouped into four layers representing the relative importance with $|\alpha| = 1,2,3,4$, respectively. We add two bar charts, one above the scatter plot and one below, to represent the Sobol and total indices of all the selected variables of interest, among which $\boldsymbol{\alpha}$ and $\boldsymbol{\beta}$ are linked to the corresponding bubble. See also Figs. 4 and 7.

A first glance at all the bubbles can quickly draw the users' attention to those big bubbles, which are also the most important ones to analyze. As for interactions, *hovering* over bubbles will highlight their corresponding links to $\boldsymbol{\alpha}$ and $\boldsymbol{\beta}$, as well as the value of the bubble as shown in Fig. 7(a). Furthermore, users can select multiple bubbles of interest by clicking, and answer questions like if they share the same attributes or subsets of $\boldsymbol{\alpha}$ or $\boldsymbol{\beta}$? Which variable contributes most to a relative importance or has overlap with other variables regarding the overall output variance? Double-clicking any bubble resets the view and new groups can be selected to verify the assumption.

Second, we also allow the user to select one or more variables for $\boldsymbol{\alpha}$ by clicking on their bars at the top as shown in Fig. 7(b) and all bubbles who share the same $\boldsymbol{\alpha}$ will be highlighted. Similarly, clicking or selecting bars from the bottom will highlight all the bubbles corresponding to $\boldsymbol{\beta}$ as shown in Fig. 7(c). In practice, different combinations of $\boldsymbol{\alpha}$ and $\boldsymbol{\beta}$ will have to be explored until finding the most important relative importance configuration. The user can further click on bubbles of interest among the highlighted ones to gain a more in-depth comparison and analysis. Eventually,

© 2021 The Author(s)
Computer Graphics Forum © 2021 The Eurographics Association and John Wiley & Sons Ltd.

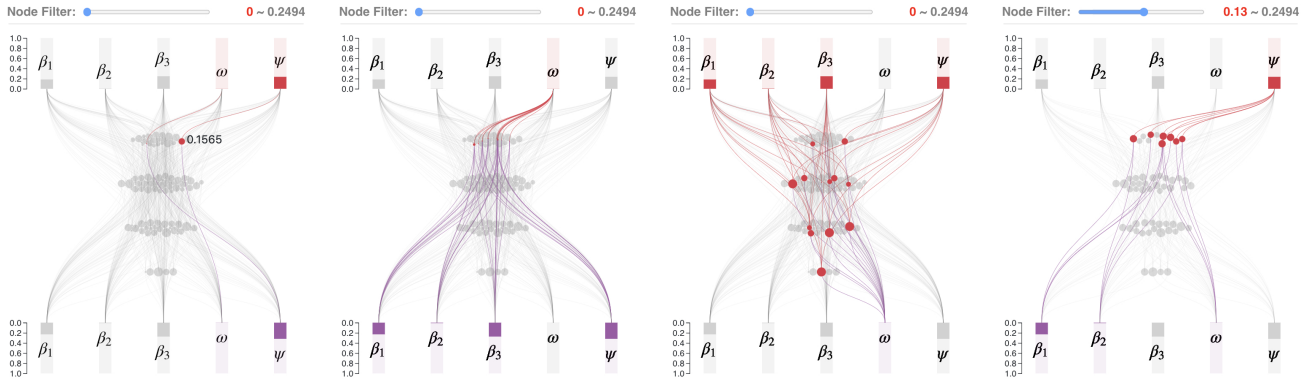

(a) hovering & clicking on bubbles (b) clicking on upper bar: $\boldsymbol{\alpha} = \{\omega\}$ (c) clicking on lower bar: $\boldsymbol{\beta} = \{\omega\}$ (d) filtering & $\boldsymbol{\alpha} = \{\psi\}$

Figure 7: *Interaction view (variables chosen: $\beta_1, \beta_2, \beta_3, \omega$, and ψ). While variable ω is heavily influenced by other variables (c), it contributes little to other variables (b). In contrast, ψ contributes significantly to other variables (a, d). We can conclude that the influence of ω itself is very small; this can be further verified in the tabular view, as S_ω is the smallest among all first-order Sobol indices.*

for iterative search and comparison steps, double-clicking any bar resets the view to the initial state.

Moreover, a filter slider is added on the top of this view so that users can easily filter out smaller relative importance values for a quick analysis, as well as uncover potentially important variables (Fig. 7(d)). Note that applying filtering can also help alleviate the potential clutter issue caused by the compact bubble layout.

One could visualize relative importances using a scatter plot with variable sized bubbles and an arc layer around to represent the two variable tuples. However, searching for bubbles which share the same variables is difficult and would require more involved interaction techniques like grouping, but further complicated interactions can reduce the effectiveness of the visual design [Mac86]. Note that our compact hourglass design looks similar to PivotPaths [DHRRD12]. However, the design focus and interaction techniques are different: PivotPaths uses linking and highlighting for information retrieval while our design uses linking to show relations and highlighting for relation comparison.

5.2. Support for User Specified Models

To further support the analysis of user-defined models (**R5**) and help for model refining, we provide an upload functionality which allows users to upload their own model by following certain instructions. Once the file is uploaded, one can perform the same visual analytical tasks as described in the preceding section.

6. Case Studies

Sensitivity visualization can be useful for a wide range of applications. We have chosen two representative model examples from different research areas to demonstrate the expressiveness and effectiveness of our system in two aspects: model understanding and model simplification.

6.1. Ebola Spread Model

Beginning in December 2013, there was a 40% fatality rate Ebola outbreak originating from Guinea, Liberia, and Sierra Leone. The virus resulted in 11,310 deaths in the area [WHO], and its spread has been the subject of several epidemiological modeling efforts [WBH*15, SYK14, RLM*14]. To assist in resource allocation in Western Africa, Diaz et al. [DCK*18] modeled the disease's infection rate using a SEIR model that depends on 8 input variables as shown in Eq. 3. Among these, *hospitalization rate (ψ)* and *proper burial rate (ω)* can easily be affected by human intervention, whereas the remaining variables depend mostly on environmental factors. They found out that ψ has a greater impact than ω in decreasing the infection rate in both Liberia and Sierra Leone, and the benefit of increasing ψ is especially acute in Sierra Leone. However, the authors only performed a first-order sensitivity analysis, i.e., disregarding any joint effects among multiple variables.

$$R_0 = \frac{\beta_1 + \frac{\beta_2 \rho_1 \gamma_1}{\omega} + \frac{\beta_3}{\gamma_2}\psi}{\gamma_1 + \psi} \tag{3}$$

In contrast, using SenVis one can easily tell how much each variable and variable set influences the output, if increasing certain variables can increase or decrease the output, and how effective such increase or decrease is. From Fig. 8, we can directly draw the same conclusions as in [DCK*18] from the ranked first-order *tabular view* that the ψ (variable 8) causes the greatest decrease of the model output while variables 2, 4 and 7 have little influence at reducing the reproduction number in either country. We also see that ψ can influence the output more in Sierra Leone than in Liberia. Further, SenVis actually shows exactly how much each of the 8 variables can affect, and either increase or decrease the model output, which makes sensitivity analysis of a specific model much easier to understand.

As argued before, knowing only the first order sensitivity indices is inadequate for decision making. Like in this case, we know that for

© 2021 The Author(s)
Computer Graphics Forum © 2021 The Eurographics Association and John Wiley & Sons Ltd.

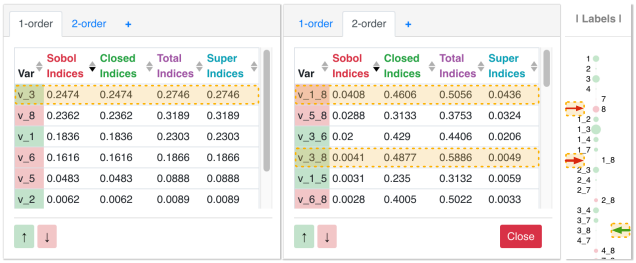

(a) Liberia

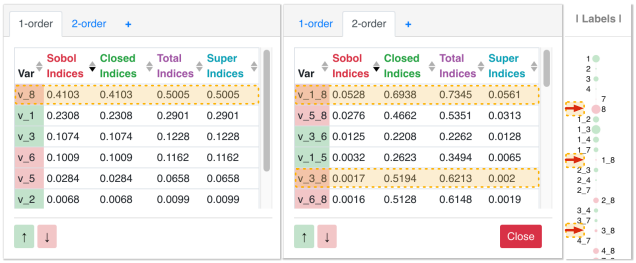

(b) Sierra Leone

Figure 8: *Tabular view for the Ebola spread model in two countries, showing both the consistent result as presented in previous research and a higher order sensitivity interpretation not previously revealed.*

both Liberia and Sierra Leone, attribute 8 can decrease the output most while attributes 1 and 3 increase the output, but we do not know if the joint effects of $\boldsymbol{\alpha} = \{1,8\}$ or $\{3,8\}$ can increase or decrease the output. By examining the 2-order *tabular view* we find that in both nations $\{1,8\}$ together will decrease the output, and in Sierra Leone $\{3,8\}$ will also decrease the output while in Liberia it will increase the output which is what we want to prevent. Additionally, users can find out how effectively single variables or variable sets can influence the output in the *Sobol view* by checking their corresponding label circles' size, and in both cases, $\{3,8\}$ influences the output more than $\{1,8\}$, as can be seen from the vertical bubble chart highlighted in Figs. 8(a) and 8(b).

6.2. Welch's Function

GSA is also useful for model simplification, i.e., removal of unimportant variables [SRV19]. As a use case we now consider *Welch's function* [WBS*92], which takes 20 variables as defined below. It includes high-order interactions and is widely regarded as a challenging model to simplify automatically.

$$\begin{aligned} f(\boldsymbol{x}) = {} & \frac{5x_{12}}{1+x_1} + 5(x_4 - x_{20})^2 + x_5 + 40x_{19}^3 - 5x_{19} + 0.05x_2 \\ & + 0.08x_3 - 0.03x_6 + 0.03x_7 - 0.09x_9 - 0.01x_{10} - 0.07x_{11} \\ & + 0.25x_{13}^2 - 0.04x_{14} + 0.06x_{15} - 0.01x_{17} - 0.03x_{18} \end{aligned} \tag{4}$$

SenVis can seamlessly reveal the model's sensitivity index structure and, in particular, distinguish all influential vs. non-influential variables. Fig. 9 shows how all important individual variables (x_4, x_5, x_{12}, x_{19}, and x_{20}) as well as the two main interaction effects ($\boldsymbol{\alpha} = \{x_{12}, x_1\}$ and $\{x_4, x_{20}\}$) are recognized. Besides, thanks to the powerful representation of the *interaction view*, we are also able to find out how each of them is affected by the other from the nonlinear relations within those two interaction groups. These insights can be crucial for model simplification, a task where traditional methods often fall short.

Specifically, in the *tabular view* (Fig. 9 (a)), all the five explicitly important variables are identified by their high Sobol indices in ①. The second-order influence of x_1 is easily discovered by ranking all total indices as shown in ②, and two groups of variable interaction $\{1,12\}$ and $\{4,20\}$, are clearly captured in the 2-order *tabular view* (③). Second, we then examine the Sobol indices relationship in the *Sobol view* (Fig. 9 (b)) where all the compositing sensitivity indices are highlighted and linked to the total donut chart after hovering on one total index. We can see that $S^T_{\{5\}}$ and $S^T_{\{19\}}$ do not have any contribution from other variables, whereas $S^T_{\{1,12\}}$ has only contributions from $S_{\{12\}}$ and $S_{\{1\}}$ (note that the link to $S_{\{1\}}$ is not shown because $S_{\{1\}} = 0$ thus the link weight is 0) and $S^T_{\{4,20\}}$ has only contribution from $S_{\{4\}}$ and $S_{\{20\}}$ (④). These relations are all consistent with the structure of Eq. 4.

Last, we can further explore the interaction effects of these six variables, which causes their totally different Sobol indices behaviors, from the *interaction view* (Fig. 9 (c)). For example, we already know that $S^T_{\{5\}}$ and $S^T_{\{19\}}$ only depend on their own Sobol indices. We can now conclude that in this case it means they have no interactions with other variables at all. Thus, if we filter out the bubbles with 0 relative importance and click on variable x_5 or x_{19} on either the upper or lower bar charts, all links related to x_5 or x_{19} disappear as illustrated in ⑤. ⑥ shows the interaction effect of x_1 and x_{12}. It tells that $R_{\{1\},\{12\}}$ is very small, i.e., very little of x_{12}'s influence is due to its interaction with x_1, while $R_{\{12\},\{1\}} = 1$, i.e., x_{12} plays a role in all of x_1's influence. The left sub-image in this widget further confirms this point: the relative importances of the intersections of x_{12} and other variables with respect to x_1 are all equal to 1. In contrast, when we did the same for checking the interaction effect of x_4 and x_{20} as shown in ⑦, we see that most of the variability of x_4 is captured by x_{20} and vice versa, showing that they have a comparable interaction effect. Furthermore, we checked the variability of the intersection of x_4 and x_{20} and it turns out to have no influence on other variables. Note that, in the second sub-image of ⑧, all the variable tuples linked by the highlighted bubbles contain x_4. In the third sub-image, all the variable tuples linked by the highlighted bubbles contain x_{20}. Thus, we can conclude that x_4 and x_{20} have strong influence towards each other but the intersection of them has no influence towards other variables, which again matches the function definition.

7. Discussion and Conclusions

We developed *SenVis*, the first Sobol-based sensitivity visualization system, to help researchers explore the most powerful variance-based GSA method. To address the prior inefficiencies of the GSA method itself, we exploit a recently developed tensor-based SA method that represents all the sensitivity indices using a highly

© 2021 The Author(s)
Computer Graphics Forum © 2021 The Eurographics Association and John Wiley & Sons Ltd.

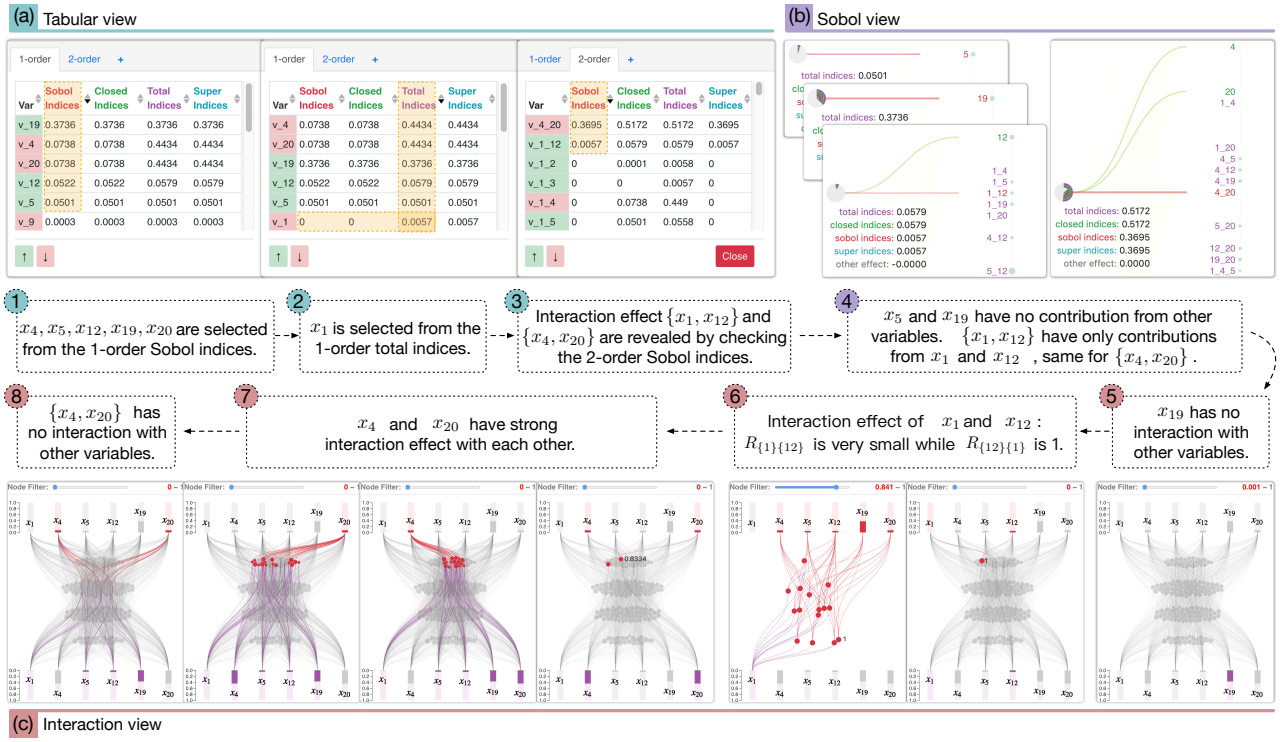

Figure 9: *Sensitivity visualization for Welch's function. Six significantly important variables are selected and their corresponding sensitivity indices and relationships are visualized in the (a) tabular, (b) Sobol, and (c) interaction views.*

effective tensor format for compact storage and fast querying at low approximation loss. The root mean squared error (RMSE) for the Ebola spread and Welch 1992 models was $1.05 \cdot 10^{-7}$ and 10^{-14}, respectively, estimated over 10^4 samples taken at random in each case. Our system is able to compute and visualize all the sensitivity indices and their derived variants for high dimensional models, as well as the relative importance of any two disjoint subsets of input variables. We further showcased the use of those metrics for detailed reasoning and understanding of the relationship of variables towards their influence to the model's output.

SenVis uses Python for the backend computations including Sobol tensor construction, sensitivity indices calculation and querying, and JavaScript for the frontend visualization interface. The reason to separate the calculation and visualization part is to benefit from doing the calculation offline and experience a smooth interaction when using the system for exploratory analysis tasks. The computation cost largely depends on the complexity of the model. To make it feasible to handle large numbers of variables, we adopted a similar strategy as in UpSet [LGS*14], that is, to limit the order of Sobol indices to 4, based on our experience that all others are almost or close to zero. For our tests, the *pre-loading* computation phase took less than 0.5*s* for models with four input variables and 5*s* at most for models up to 10 input variables, which ensures a smooth user interaction. Note that the order cap can freely be chosen in our system. Our code is available on GitHub [Yan].

Even though our system can handle a large range of models, it has some limitations. First, it assumes that the input variables are mutually independent or can be freely set by the user (as in an experimental design). Second, our diagrams are only applicable to models having a few dozens of dimensions at most. For even higher-dimensional spaces, say $N \geq 30$, the current frontend will suffer from scalability issues that other related set visualization techniques have as well [AMA*14]. One possible solution to ease this limitation is to exclude the variables with smaller total indices (that is, unimportant variables) in the pre-loading phase. Note that our Python computation backend has been tested to work with larger number of variables, however, some JavaScript operations in the frontend are currently limited in processing the incoming data.

Furthermore, we plan to deploy our visualization system on a publicly accessible server and make it usable to researchers and practitioners in two groups: (a) domain experts in disciplines that can benefit from GSA-driven tasks (e.g., in the life and medical sciences, engineering, and other areas using mathematical modeling), and (b) researchers in GSA theory and algorithms, so that they can easily grasp and explore the influence and interactions of large, potentially complex mathematical models and use them as a baseline.

Acknowledgments

The authors would like to thank Dr. Enrique G. Paredes for contributing Fig. 1.

© 2021 The Author(s)
Computer Graphics Forum © 2021 The Eurographics Association and John Wiley & Sons Ltd.

References

[AAMH13] ALSALLAKH B., AIGNER W., MIKSCH S., HAUSER H.: Radial sets: Interactive visual analysis of large overlapping sets. *IEEE Transactions on Visualization and Computer Graphics 19* (2013), 2496–2505. 3

[AMA*14] ALSALLAKH B., MICALLEF L., AIGNER W., HAUSER H., MIKSCH S., RODGERS P.: Visualizing sets and set-typed data: State-of-the-art and future challenges. In *EuroVis State of the Art Reports* (June 2014), pp. 1–21. 3, 10

[BEK15] BIGONI D., ENGSIG-KARUP A.: *Uncertainty Quantification With Applications to Engineering Problems*. PhD thesis, Technical University of Denmark, 2015. 2

[BHJ*14] BONNEAU G.-P., HEGE H.-C., JOHNSON C. R., OLIVEIRA M. M., POTTER K., RHEINGANS P., SCHULTZ T.: Overview and state-of-the-art of uncertainty visualization. In *Scientific Visualization: Uncertainty, Multifield, Biomedical, and Scalable Visualization* (2014), pp. 3–27. 3

[BLLS16] BISWAS A., LIN G., LIU X., SHEN H.-W.: Visualization of time-varying weather ensembles across multiple resolutions. *IEEE transactions on visualization and computer graphics 23*, 1 (2016), 841–850. 3

[BRP16] BALLESTER-RIPOLL R., PAJAROLA R.: Tensor decomposition methods in visual computing. *IEEE Vis. Tutorials* (2016). 3

[BRPP18] BALLESTER-RIPOLL R., PAREDES E. G., PAJAROLA R.: Tensor algorithms for advanced sensitivity metrics. *SIAM/ASA Journal on Uncertainty Quantification 6*, 3 (2018), 1172–1197. 2

[BRPP19] BALLESTER-RIPOLL R., PAREDES E. G., PAJAROLA R.: Sobol tensor trains for global sensitivity analysis. *Reliability Engineering and System Safety 183* (March 2019), 311–322. 2, 3, 4, 5

[DCK*18] DIAZ P., CONSTANTINE P. G., KALMBACH K., JONES E., PANKAVICH S.: A modified SEIR model for the spread of Ebola in western Africa and metrics for resource allocation. *Applied Mathematics and Computation 324* (2018), 141–155. 8

[DHRRD12] DORK M., HENRY RICHE N., RAMOS G., DUMAIS S.: PivotPaths: Strolling through faceted information spaces. *IEEE Transactions on Visualization and Computer Graphics 18*, 12 (Dec. 2012), 2709–2718. 3, 8

[DKLM14] DOLGOV S. V., KHOROMOSKIJ B. N., LITVINENKO A., MATTHIES H. G.: Computation of the response surface in the tensor train data format. arXiv:1406.2816, 2014. 2

[ES81] EFRON B., STEIN C.: The jackknife estimate of variance. *Ann. Statist. 9*, 3 (05 1981), 586–596. 2

[FRM13] FRUTH J., ROUSTANT O., MUEHLENSTAEDT T.: The fanovaGraph package: Visualization of interaction structures and construction of block-additive kriging models. *HAL preprint 00795229* (2013). 3

[Hol06] HOLTEN D.: Hierarchical edge bundles: Visualization of adjacency relations in hierarchical data. *IEEE Transactions on visualization and computer graphics 12*, 5 (2006), 741–748. 6

[Hoo04] HOOKER G.: Discovering additive structure in black box functions. In *ACM SIGKDD International Conference on Knowledge Discovery and Data Mining* (August 2004), pp. 575–580. 4

[HQC*19] HULLMAN J., QIAO X., CORRELL M., KALE A., KAY M.: In pursuit of error: A survey of uncertainty visualization evaluation. *IEEE Transactions on Visualization and Computer Graphics 25*, 1 (2019), 903–913. 2

[IL15] IOOSS B., LEMAÎTRE P.: *A Review on Global Sensitivity Analysis Methods*. Springer US, Boston, MA, 2015, pp. 101–122. 1, 2

[KB09] KOLDA T. G., BADER B. W.: Tensor decompositions and applications. *SIAM Review 51*, 3 (2009), 455–500. 3

[KS16] KONAKLI K., SUDRET B.: Global sensitivity analysis using low-rank tensor approximations. *Reliability Engineering & System Safety 156* (2016), 64 – 83. 2

[KSV*15] KERSAUDY P., SUDRET B., VARSIER N., PICONC O., WIART J.: A new surrogate modeling technique combining Kriging and polynomial chaos expansions – Application to uncertainty analysis in computational dosimetry. *Journal of Computational Physics 286* (2015), 103–117. 2

[LGS*14] LEX A., GEHLENBORG N., STROBELT H., VUILLEMOT R., PFISTER H.: UpSet: Visualization of intersecting sets. *IEEE Transactions on Visualization and Computer Graphics 20*, 12 (2014), 1983–1992. 3, 10

[Mac86] MACKINLAY J.: Automating the design of graphical presentations of relational information. *ACM Trans. Graph. 5*, 2 (1986), 110–141. 8

[Ose11] OSELEDETS I. V.: Tensor-train decomposition. *SIAM Journal on Scientific Computing 33*, 5 (September 2011), 2295–2317. 3

[Owe13] OWEN A. B.: Variance components and generalized Sobol' indices. *SIAM Journal on Uncertainty Quantification 1*, 1 (2013), 19–41. 2, 4

[Owe14] OWEN A. B.: Sobol' indices and shapley value. *SIAM/ASA Journal on Uncertainty Quantification 2*, 1 (2014), 245–251. 2

[PRJ12] POTTER K., ROSEN P., JOHNSON C. R.: From quantification to visualization: A taxonomy of uncertainty visualization approaches. In *IFIP Advances in Information and Communication Technology* (2012), vol. 377, pp. 226–249. 2

[QHS*05] QUEIPO N. V., HAFTKA R. T., SHYY W., GOEL T., VAIDYANATHAN R., TUCHER P. K.: Surrogate-based analysis and optimization. *Progress in Aerospace Sciences 41* (2005), 1–28. 2

[Rai14] RAI P.: *Sparse Low Rank Approximation of Multivariate Functions – Applications in Uncertainty Quantification*. Doctoral thesis, Ecole Centrale Nantes, Nov. 2014. 2

[RHF05] RIEHMANN P., HANFLER M., FROEHLICH B.: Interactive sankey diagrams. In *IEEE Symposium on Information Visualization, 2005. INFOVIS 2005.* (2005), pp. 233–240. 6

[RLM*14] RIVERS C. M., LOFGREN E. T., MARATHE M., EUBANK S., LEWIS B. L.: Modeling the impact of interventions on an epidemic of Ebola in Sierra Leone and Liberia. *PLoS currents 6* (2014). 8

[SMDS14] SADANA R., MAJOR T., DOVE A., STASKO J.: Onset: A visualization technique for large-scale binary set data. *IEEE transactions on visualization and computer graphics 20*, 12 (2014), 1993–2002. 3, 6

[Sob90] SOBOL' I. M.: Sensitivity estimates for nonlinear mathematical models (in Russian). *Mathematical Models 2* (1990), 112–118. 1, 2

[SRA*08] SALTELLI A., RATTO M., ANDRES T., CAMPOLONGO F., CARIBONI J., GATELLI D., SAISANA M., TARANTOLA S.: *Global Sensitivity Analysis: The Primer*. John Wiley & Sons, Ltd., 2008. 1, 2

[SRV19] SPAGNOL A., RICHE R. L., VEIGA S. D.: Global sensitivity analysis for optimization with variable selection. *SIAM/ASA Journal on Uncertainty Quantification 7*, 2 (2019), 417–443. 9

[STCR04] SALTELLI A., TARANTOLA S., CAMPOLONGO F., RATTO M.: *Sensitivity Analysis in Practice: A Guide to Assessing Scientific Models*. Halsted Press, New York, NY, USA, 2004. 2, 4

[Sud08] SUDRET B.: Global sensitivity analysis using polynomial chaos expansions. *Reliability Engineering and System Safety 93*, 7 (2008), 964 – 979. 1, 2

[SYK14] SHAMAN J., YANG W., KANDULA S.: Inference and forecast of the current West African Ebola outbreak in Guinea, Sierra Leone and Liberia. *PLoS currents 6* (2014). 8

[VBP*19] VALDIVIA P., BUONO P., PLAISANT C., DUFOURNAUD N., FEKETE J.-D.: Analyzing dynamic hypergraphs with parallel aggregated ordered hypergraph visualization. *IEEE Transactions on Visualization and Computer Graphics to appear* (August 2019). 3

[Wat02] WATTENBERG M.: Arc diagrams: Visualizing structure in strings. In *IEEE Symposium on Information Visualization, 2002. INFOVIS 2002.* (2002), pp. 110–116. 6

© 2021 The Author(s)
Computer Graphics Forum © 2021 The Eurographics Association and John Wiley & Sons Ltd.

[WBH*15] WEBB G., BROWNE C., HUO X., SEYDI O., SEYDI M., MAGAL P.: A model of the 2014 Ebola epidemic in West Africa with contact tracing. *PLoS currents 7* (2015). 8

[WBS*92] WELCH W. J., BUCK R. J., SACKS J., WYNN H. P., MITCHELL T. J., MORRIS M. D.: Screening, predicting, and computer experiments. *Technometrics 34*, 1 (1992), 15–25. 9

[WHO] WORLD HEALTH ORGANIZATION: Situation report: Ebola virus disease - 10 June 2016. https://apps.who.int/iris/bitstream/handle/10665/208883/ebolasitrep_10Jun2016_eng.pdf. 8

[WWO*16] WU Z., WANG D., OKOLO P. N., HU F., ZHANG W.: Global sensitivity analysis using a Gaussian radial basis function metamodel. *Reliability Engineering and System Safety 154* (2016), 171–179. 2

[WWO*17] WU Z., WANG D., OKOLO P. N., ZHAO K., ZHANG W.: Efficient space-filling and near-orthogonality sequential Latin hypercube for computer experiments. *Computer Methods in Applied Mechanics and Engineering 324* (2017), 348–365. 2

[Yan] YANG H.: SenVis: A visualization tool for sensitivity analysis. Visualization and MultiMedia Lab, University of Zürich, https://github.com/visangela/SenVis/. 10

© 2021 The Author(s)
Computer Graphics Forum © 2021 The Eurographics Association and John Wiley & Sons Ltd.